ELSEVIER

Chemical Engineering Journal 84 (2001) 381–388

Chemical Engineering Journal

www.elsevier.com/locate/cej

Heat transfer in gas–liquid–liquid three-phase direct-contact exchanger

Zhang Peng [a,*], Wang Yiping [a], Guo Cuili [a], Wang Kun [b]

[a] *School of Chemical Engineering and Technology, Tianjin University, P.O. Box 699, Tianjin 300072, China*
[b] *Department of Fine Chemicals, Jilin Institute of Chemical Technology, Jilin 132022, China*

Received 15 December 1999; received in revised form 18 December 2000; accepted 20 December 2000

Abstract

The heat transfer to dispersed droplets in an immiscible continuous phase is studied for the *n*-pentane–water system. The gas–liquid–liquid three-phase section of the exchanger is divided into two stages, where the volumetric heat transfer coefficients are developed, respectively. These models take into account the evaporation of continuous phase water into the dispersed phase and the two-phase droplets break-up. The calculated results showed good agreement with the experimental values.

Keywords: Gas–liquid–liquid three-phase flow; Direct-contact heat transfer; Volumetric heat transfer coefficient

1. Introduction

Direct-contact heat transfer between two immiscible liquids has been one of the most popular research projects in heat transfer field. Because its many advantages such as relative simplicity of design, fewer scaling problems, higher heat transfer coefficient (about 20–100 times that of single-phase flow [1]), having no metallic heat transfer surfaces that are prone to corrosion and fouling, and the capacity to operate at relatively small temperature driving forces, it has been utilized in many industrial fields including water desalination [2], crystallization [3,4], solar and geothermal power [5]. It is therefore necessary to know about the heat transfer characteristics of dispersed phase droplets in a continuous medium. Due to the complexity of the multiphase flow in exchangers, the heat exchange performance has often been expressed in terms of the volumetric heat transfer coefficient, h_v. The volumetric heat transfer coefficient in a column can be determined experimentally without regard to the interfacial area held in the column at each instant [6]. However, its value thus determined must be specific to the operational conditions as well as to the geometry and the dimensions of the column. Thus, it is important to develop a general method that enables us to predict the volumetric heat transfer coefficient, depending only on our common knowledge of fluid mechanics and heat transfer in multiphase systems. Along this line of investigation, Smith et al. [7] presented an explicit, closed-form expression for the volumetric heat transfer coefficient. The drawback of the model is that it assumes a continuous phase that is stagnant and uniform in temperature. Core and Mulligan [8] presented a population balance analysis of a bath evaporator, assuming the evaporation of drops in a uniform but transient temperature field and a negligible droplet coalescence.

This paper studies the heat transfer in a parallel flow exchanger and discusses the effects of some operational parameters on the volumetric heat transfer coefficient. Some expressions take account of the possible coalescence and break-up of the droplets. The expressions may improve our insight into the dependencies of the total heat transfer performance of exchangers on individual operational parameters and, indirectly, on the exchanger design.

2. Modeling

The volumetric heat transfer coefficient, h_v, as an important parameter in the process of direct-contact heat transfer, is often used to express the heat exchange performance. It is defined as

$$h_v = \frac{Q}{AH\,\Delta T} \tag{1}$$

where Q is the rate of heat supplied from the continuous phase to the evaporating dispersed phase in an exchanger whose cross-sectional area and effective height for the heat exchange are A and H, respectively. The temperature

* Corresponding author. Tel.: +86-22-27401679 (R), +86-22-27407311 (O).
E-mail addresses: zh-peng@freemail.online.tj.cn, zpwk@263.net (Z. Peng).

1385-8947/01/$ – see front matter
PII: S1385-8947(01)00131-0

Nomenclature

A	cross-sectional area of the exchanger (m^2)
A_d	droplet surface area (m^2)
C_p	specific heat capacity ($kJ\,kg^{-1}\,K^{-1}$)
d_h	orifice diameter (m)
D	equivalent spherical diameter of drop, two-phase droplet or vapor bubble (m)
D_r	inside diameter of the exchanger (m)
f_w	wall friction coefficient
g	gravitational constant ($m^2\,s^{-1}$)
h_d	single droplet heat transfer coefficient based on surface area of spherical two-phase droplet ($kW\,m^{-2}\,K^{-1}$)
h_{mv}	average volumetric heat transfer coefficient ($kW\,m^{-3}\,K^{-1}$)
h_v	local volumetric heat transfer coefficient ($kW\,m^{-3}\,K^{-1}$)
Δh	reading of a manometer (m)
H	exchanger height effective for heat exchange (m)
H_v	value of H for complete vaporization of dispersed phase (m)
ΔH	height difference (m)
$\Delta_r H$	latent heat of evaporation ($kJ\,kg^{-1}$)
m	mass flow rate ($kg\,s^{-1}$)
M	molecular weight ($g\,mol^{-1}$)
n_d	number density of two-phase droplets (m^{-3})
n_h	number of orifices in the distributor
Nu	Nusselt number ($=h_d D/\kappa$)
P	pressure (kPa)
Pe	Peclet number ($=U_r D/a$)
P^s	saturated steam pressure (kPa)
ΔP	pressure difference (kPa)
Q	rate of heat transfer ($kJ\,s^{-1}$)
Q_e	rate of heat released to the environment ($kJ\,s^{-1}$)
R	gas constant ($8.314\,J\,mol^{-1}\,K^{-1}$)
T	temperature (K)
ΔT	temperature difference between continuous and dispersed phases (K)
u	superficial velocity ($m\,s^{-1}$)
U	rise velocity of droplet relative to a coordinate fixed to exchanger ($m\,s^{-1}$)
U_r	relative velocity between continuous and dispersed phases ($m\,s^{-1}$)
V	volume flow rate (or volume) ($m^3\,s^{-1}$)
Z	axial displacement (m)

Greek letters

α	thermal diffusivity ($m^2\,s^{-1}$)
ε	energy dissipation per unit mass and time ($m^2\,s^{-3}$)
ε_g	gas hold-up (or dispersed phase volume fraction) ($m^3\,m^{-3}$)
κ	thermal conductivity ($W\,m^{-1}\,K^{-1}$)
ρ	density ($kg\,m^{-3}$)
σ	surface tension ($N\,m^{-1}$)

Subscripts

av	average
c	continuous phase
cv	continuous phase vapor
cw	water at room temperature
CCl_4	carbon tetrachloride
d	dispersed phase
dl	dispersed phase liquid
dv	dispersed phase vapor
dvm	vapor phase inside the droplet
g	gas
in	inlet
m	average of continuous and dispersed phases
max	maximum
min	minimum
out	outlet
top	top of the exchanger
0	initial value

difference between the two phases, ΔT, may be considerably nonuniform along the column axis.

Thus, the volumetric heat transfer coefficient in the gas–liquid–liquid three-phase section can be determined according to this definition.

Before deriving the volumetric heat transfer coefficients, some reasonable assumption should be introduced for convenience. (1) The liquid–vapor two-phase droplet is regarded as a sphere whose equivalent spherical diameter is D. (2) The vapor is always saturated by the steam evaporating from the vapor–liquid interface. The total pressure is the sum of partial pressure of *n*-pentane vapor and steam. (3) The vapor is regarded as an ideal gas. (4) The coalescence and fragmentation of two-phase droplets have no influences on the distribution of the gas hold-up along the column height.

According to the principle that the dispersed droplets are fragmented by the turbulent flow of continuous phase, the maximum diameter of the dispersed droplets for *n*-pentane–water system can be determined by the following relation [9]:

$$D_{max} = 1.14 \left(\frac{\sigma_c}{\rho_c}\right)^{0.6} \varepsilon^{-0.4} \tag{2}$$

where the energy dissipation per unit mass and time, ε, is written as [10]

$$\varepsilon = \frac{2 f_w u_c^3}{D_r} \tag{3}$$

where f_w is a wall friction coefficient that can be calculated by [11]

$$f_w = 0.0486 \left(\frac{\sqrt{gD_r}}{u_c}\right)^{1.1} \sqrt{\varepsilon_{g_{av}}} \tag{4}$$

where $\varepsilon_{g_{av}}$ is the mean gas hold-up. The range of variables in Eq. (4) is

$$\varepsilon_{g_{av}} > 0, \qquad 0 < \frac{u_c}{\sqrt{gD_r}} < 1$$

The gas hold-up, ε_g, can be calculated by the measured pressure at the different height of the exchanger. Considering the pressure balance between the two points that the pressure difference is ΔP and the height difference is ΔH, we have

$$(\rho_c(1-\varepsilon_g) + \rho_{dvm}\varepsilon_g) g\,\Delta H = \Delta P \tag{5}$$

For $\rho_{dvm} \ll \rho_c$, we get

$$\varepsilon_g = 1 - \frac{\Delta P}{\rho_c g\,\Delta H} \tag{6}$$

Then the mean gas hold-up can be calculated by

$$\varepsilon_{g_{av}} = \frac{\sum \varepsilon_{g_i}\Delta H_i}{H_v} \tag{7}$$

The relative velocity between continuous and dispersed phases, U_r, tends to change slowly, so that it can be regarded as approximately a constant represented by its mean value in the column. Peng et al. [12] and Mori [13] had verified that this assumption is reasonable. Then the relative velocity can be calculated by

$$U_r = \frac{u_d}{\varepsilon_{g_{av}}} - \frac{u_c}{1-\varepsilon_{g_{av}}} \tag{8}$$

The most fundamental assumption in the present model is that the heat transfer to each drop, taking the form of a liquid–vapor two-phase droplet in the course of evaporation, is described by the same heat transfer correlation as that established for single-drop evaporation [14]. We simply substitute a mean relative velocity between the continuous and dispersed phases in the column for the droplet velocity used in the correlation. The correlation is given by

$$Nu_c = \frac{h_d D}{\kappa_c} = 0.169 Pe^{1/2} \tag{9}$$

It is assumed that there are two stages in the process of droplets evaporating and buoyantly rising through the continuous liquid. In the first stage the interactions of dispersed droplets are so weak that it can be assumed that the individual droplets behave independently of one another and there is no coalescence and fragmentation between them. Thus, the number density of droplets in this stage must be constant, that is $n_d = n_{d0}$. With the two-phase droplets rising, their diameters increase. At the second stage the droplets reach Z_{max} in height and D_{max} in diameter. In this stage the droplets affect each other and begin to coalesce or fragment. It is assumed that the diameter of droplets keeps the constant value of D_{max}, while the number density of the droplets varies with the height in the second stage.

2.1. Volumetric heat transfer coefficients in the first stage ($Z < Z_{max}$)

The local volumetric heat transfer coefficient at an elevation Z above the distributor, where the diameter of each droplet arrives at D, is written as

$$h_v = n_{d0}\pi D^2 h_d \tag{10}$$

where h_d denotes the surface heat transfer coefficient specified by Eq. (9) and n_{d0}, the initial droplet number density can be calculated by using

$$n_{d0} = \frac{u_d}{(1/6)\pi D_0^3 U_{d0}} \tag{11}$$

where U_{d0} is the initial velocity of the dispersed phase. Because the mass of the dispersed phase entering the distributor per unit time is equal to that leaving the distributor, U_{d0} can be calculated by using

$$U_{d0} = \frac{4V_d}{\pi n_h d_h^2} \tag{12}$$

The initial drop diameter depends mainly on the orifice velocity and orifice diameter [15]. For pentane–water system it can be calculated by

$$D_0 = 0.00307 U_{d0}^{0.35} d_h^{0.72} \tag{13}$$

The variable D in Eq. (10) needs to be replaced by the axial displacement, Z. For this purpose, we consider the energy balance in a differential element of volume whose height is dZ. Thus, the net mass of vapor increasing per unit time in the differential element of volume is

$$\mathrm{d}m = m_{out} - m_{in} = \rho_{dvm} n_{d0} U_r A\,\mathrm{d}V_{dvm} \tag{14}$$

In addition, the mass balance of *n*-pentane for each droplet is

$$\left(\tfrac{1}{6}\pi\right) D_0^3 \rho_{dl} = \rho_{dv} V_{dvm} + \rho_{dl}\left(\tfrac{1}{6}\pi D^3 - V_{dvm}\right) \tag{15}$$

that is

$$V_{dvm} = \frac{1}{6}\pi \frac{\rho_{dl}}{\rho_{dl} - \rho_{dv}}(D^3 - D_0^3) \tag{16}$$

Substituting Eq. (16) into Eq. (14) yields

$$\mathrm{d}m = \tfrac{1}{2}\pi D^2 Cm_1 A n_{d0} U_r\,\mathrm{d}D \tag{17}$$

where

$$Cm_1 = \frac{\rho_{dl}\rho_{dvm}}{\rho_{dl} - \rho_{dv}} \tag{18}$$

So the rate of heat transfer from the continuous phase to the dispersed phase is given by

$$\mathrm{d}Q = \mathrm{d}m\,\Delta_r H_m = \tfrac{1}{2}\pi D^2\,\Delta_r H_m\, Cm_1 A n_{d0} U_r\,\mathrm{d}D \tag{19}$$

Because the continuous and dispersed phase vapors in the two-phase droplets are always in a saturated state, the average density of vapor inside the droplets, ρ_{dvm}, and

the average latent heat of evaporation, $\Delta_r H_m$, in the above equations can be calculated by the following equations:

$$\rho_{dvm} = \frac{M_d(P - P_c^s)}{M_m P}\rho_{dv} + \frac{M_c P_c^s}{M_m P}\rho_{cv} \quad (20)$$

$$\Delta_r H_m = \frac{M_d(P - P_c^s)}{M_m P}\Delta_r H_d + \frac{M_c P_c^s}{M_m P}\Delta_r H_c \quad (21)$$

$$M_m = \frac{P - P_c^s}{P}M_d + \frac{P_c^s}{P}M_c \quad (22)$$

where P_c^s is the saturated steam pressure of water that can be determined by the average temperature.

In addition, according to the convective heat transfer equation, the rate of heat transfer, dQ, can also be written as

$$dQ = h_d \pi D^2 n_{d0}\,\Delta T\, A\, dZ \quad (23)$$

Combining Eq. (19) with Eq. (23), we have the following relation:

$$\frac{dZ}{dD} = \frac{\Delta_r H_m Cm_1 U_r}{2h_d\,\Delta T} \quad (24)$$

Rearranging Eq. (9) yields

$$h_d = Cm_2 U_r^{0.5} D^{-0.5} \quad (25)$$

where

$$Cm_2 = 0.169\kappa_c \alpha_c^{-0.5} \quad (26)$$

Substituting Eq. (25) into Eq. (24), we obtain

$$D^{0.5}\,dD = Cm_3\,\Delta T\, U_r^{-0.5}\,dZ \quad (27)$$

where

$$Cm_3 = \frac{2Cm_2}{\Delta_r H_m\, Cm_1} \quad (28)$$

The boundary conditions are $Z = 0$, $D = D_0$; $Z = Z$, $D = D$. Here we introduce the assumption of linear distribution of ΔT, the temperature difference between continuous and dispersed phases, which seems to be a reasonable compromise for eliminating the complexity [13,16]. So it is written as

$$\Delta T = \Delta T_{min} + \frac{(\Delta T_{max} - \Delta T_{min})(H_v - Z)}{H_v} \quad (29)$$

where H_v can be determined by the distributions of the measured temperature which are shown in Fig. 1. In the figure, H_v is the height where the decrease of the temperature starts to become inconsiderable. Substituting Eq. (29) into Eq. (27) and integrating the resultant equation, we have

$$D = \left\{ D_0^{1.5} + 1.5Cm_3 U_r^{-0.5} Z \times \left[\Delta T_{min} + (\Delta T_{max} - \Delta T_{min})\left(1 - \frac{Z}{2H_v}\right)\right]\right\}^{1/1.5} \quad (30)$$

Substituting Eqs. (30) and (25) into Eq. (10), the resultant expression of h_v is

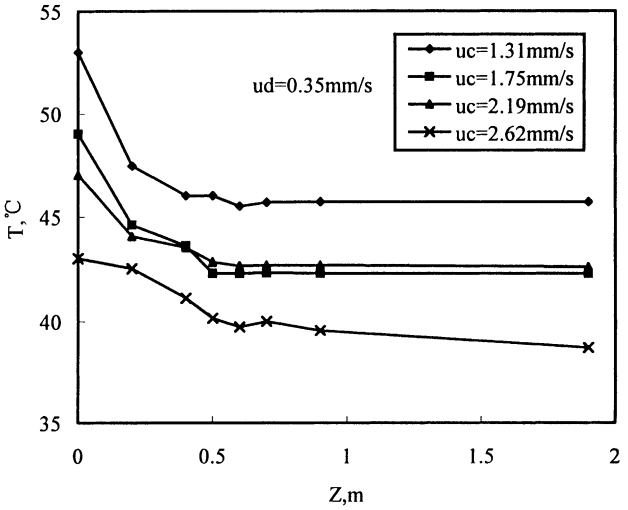

Fig. 1. Variation of the measured temperature with the exchanger height.

$$h_v = n_{d0}\pi Cm_2 U_r^{0.5}\left\{ D_0^{1.5} + 1.5Cm_3 U_r^{-0.5} Z \times \left[\Delta T_{min} + (\Delta T_{max} - \Delta T_{min})\left(1 - \frac{Z}{2H_v}\right)\right]\right\} \quad (31)$$

The average volumetric heat transfer coefficient from the distributor to the height Z, which is defined by Eq. (1), is related to h_d as

$$h_{mv}(Z) = \frac{1}{Z\,\Delta T_{av}}\int_{D_0}^{D} A_d n_d h_d\,\Delta T \frac{dZ}{dD}\,dD \quad (32)$$

With the substitution of Eq. (24) into Eq. (32), followed by a rearrangement, the average volumetric heat transfer coefficient in the first stage is obtained as

$$h_{mv}(Z) = \frac{\pi n_{d0} Cm_1\,\Delta_r H_m\, U_r D^3}{6Z\,\Delta T_{av}} \quad (33)$$

2.2. Volumetric heat transfer coefficients in the second stage ($Z > Z_{max}$)

In this stage the droplet number density, n_d, can be calculated by using

$$n_d = n_{d0}\left(\frac{D}{D_{max}}\right)^3 \quad (34)$$

where D is the diameter that each two-phase droplet would be if there is no coalescence and fragmentation in the exchanger.

The local volumetric heat transfer coefficient can be expressed as

$$h_v = n_d \pi D_{max}^2 h_d \quad (35)$$

Substituting Eqs. (25) and (34) into Eq. (35) yields

$$h_v = n_{d0}\pi Cm_2 U_r^{0.5} D_{max}^{-1.5} D^3 \quad (36)$$

Substituting Eq. (30) into Eq. (36), the resultant expression of the local volumetric heat transfer coefficient, h_v, is

$$h_v = n_{d0}\pi Cm_2 U_r^{0.5} D_{max}^{-1.5} \left\{ D_0^{1.5} + 1.5Cm_3 U_r^{-0.5} Z \times \left[\Delta T_{min} + (\Delta T_{max} - \Delta T_{min}) \left(1 - \frac{Z}{2H_v} \right) \right] \right\}^2 \quad (37)$$

According to Eq. (32), the average volumetric heat transfer coefficient is written as

$$h_{mv}(Z) = \frac{1}{Z\,\Delta T_{av}} \left(\int_{D_0}^{D_{max}} A_d n_{d0} h_d\, \Delta T \frac{dZ}{dD}\, dD + \int_{D_{max}}^{D} A_d n_d h_d\, \Delta T \frac{dZ}{dD}\, dD \right) \quad (38)$$

Substituting Eqs. (24) and (34) into Eq. (38) and integrating the resultant equation yields

$$h_{mv}(Z) = \frac{\pi n_{d0} Cm_1\, \Delta_r H_m\, U_r}{2Z\,\Delta T_{av}} \times \left(\frac{D_{max}^3 - D_0^3}{3} + \frac{D^4 - D_{max}^4}{4D_{max}} \right) \quad (39)$$

3. Experiments

3.1. Description of the experiment

The experimental setup is shown schematically in Fig. 2. It consists of a direct-contact heat exchanger, hot water supply system, dispersed phase supply system and condensation system. The exchanger is made of plexiglass with an inside diameter of 90 mm and a length of 2000 mm. On both sides of the exchanger there are 20 holes with a diameter of 8 mm each and which are used for measuring the temperature and pressure.

n-Pentane is used as the dispersed fluid. It is injected into the exchanger from a distributor located at the bottom of the exchanger. The dispersed phase liquid is supplied to the distributor through a tube from a supply tank. The distributor is

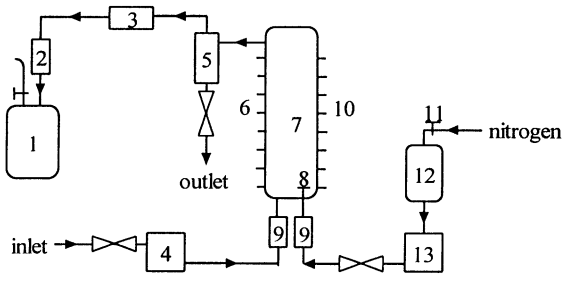

Fig. 2. Schematic diagram of experimental setup: 1, storage tank; 2, cold trap; 3, condenser; 4, water heater; 5, gas-liquid separator; 6, holes for measuring pressure; 7, direct-contact exchanger; 8, distributor; 9, rotameter; 10, holes for measuring temperature; 11, pressure regulator; 12, dispersed liquid supply tank; 13, constant temperature bath.

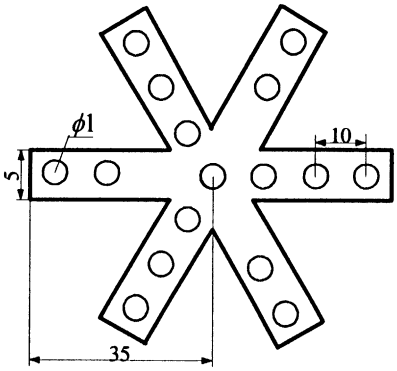

Fig. 3. Configuration of the distributor.

70 mm in diameter. The number of orifices in it is 16 and the orifice diameter is 1 mm. The arrangement of holes in the distributor is shown in Fig. 3. The supply tank is pressurized by using nitrogen and the pressure is kept constant by using a pressure regulator. The dispersed phase flow rate is measured by using a rotameter. The dispersed phase vapor that comes from the top of the column is collected from the gas–liquid separator and condensed in a water-cooled, tube-in-shell condenser and a cold trap with water–ice mixture as the medium. The condensate is collected in a storage tank.

Hot water is supplied to the exchanger from the bottom when it is heated to the given temperature in the heater. The water flow rate is measured by using a rotameter.

3.2. Operation of the experiment

The experiment is conducted as follows. Water is heated in the constant-temperature bath to the desired temperature that is high enough to make the dispersed phase evaporate completely. The dispersed phase liquid supply tank is pressurized to 200 kPa by using a nitrogen cylinder and a pressure regulator. Pentane is heated in the constant-temperature bath and then enters the exchanger from the bottom through a distributor and flows upward in droplet form while vaporizing. The heat transfer process progressively reduces the water temperature. The evaporation is allowed to take place until the dispersed phase liquid has evaporated completely. The vapor escapes from the top of the exchanger.

Temperature measurements are accomplished with the use of thermometers (the measuring scale is 0–100°C and the measuring precision is 0.01°C). The experiments have indicated that the decline of the temperature is mainly in the lower part of the exchanger. So eight thermometers are set at the positions of 0.1, 0.2, 0.4, 0.5, 0.6, 0.7, 0.9, 1.9 m and a thermometer is used to measure the inlet water temperature. Each thermometer is located at the center of a cross-section. Because of the presence of the strong turbulence and mixing during the evaporation process, the measured temperature can reasonably represent the average temperature of a cross-section. Furthermore, the measurement can be

Table 1
Conditions of experimental operations

T_{c0} (°C)	T_{d0} (°C)	P_{top} (kPa)	$u_c \times 10^3$ ($m\,s^{-1}$)	$u_d \times 10^4$ ($m\,s^{-1}$)
40.0–60.0	25.00	120	0.8–3.0	1.5–7.5

regarded as the temperature of the continuous phase. The reasons are (1) the hold-up ratio of continuous phase is much higher than that of dispersed phase in the exchanger; (2) most parts in the droplet are full of vapor and (3) the thermal conductivity of liquid is much higher than that of gas. So the heat transferring to the thermal sensor is mainly from the continuous phase. And the effect from the dispersed phase can be neglected. So did many scholars [7,8,15]. The temperature of the dispersed phase is its saturation temperature.

The average gas hold-up in the exchanger is determined by the measured pressure. Seven U-shaped glass-pipe manometers are used to measure the static pressure within the exchanger. The static pressure is measured at the heights of 0.1, 0.2, 0.4, 0.5, 0.6, 0.7, 0.9, 1.9 m. The indicator is carbon tetrachloride (CCl_4). But mercury is used as the indicator in the highest manometer because of the bigger pressure difference. If the reading of a manometer is Δh and the height difference between the two points connected to the manometer is ΔH, the static pressure difference can be calculated by the following equation:

$$\Delta P = \rho_{cw} g\,\Delta H - (\rho_{CCl_4} - \rho_{cw}) g\,\Delta h \tag{40}$$

Then the average gas hold-up between the two points can be calculated by Eq. (6).

A great deal of data were collected over a period of 3 months [12]. It indicated that the uncertainty in the experimental measurements might lead to errors in the calculation of volumetric heat transfer coefficient (defined by Eq. (41)) of 10%. The errors are mainly caused by the following reasons. The pressure measurements are only accurate within 6% of the relative error due to the undulation of the indicator level. The temperature measurements may involve as much as 3% of the relative error due to the effect of the dispersed phase. And the maximum error in the determination of H_v is about 5%. The reproducibility of the data was checked and found to be better than the uncertainty in the measurements.

3.3. Operational conditions of the experiment

The experiment is repeated by varying the T_{c0}, u_c, u_d to study their effects on the volumetric heat transfer coefficient. The conditions of experimental operations are shown in Table 1.

4. Results and discussions

Considering the energy balance in an element of volume whose height is ΔZ, we get

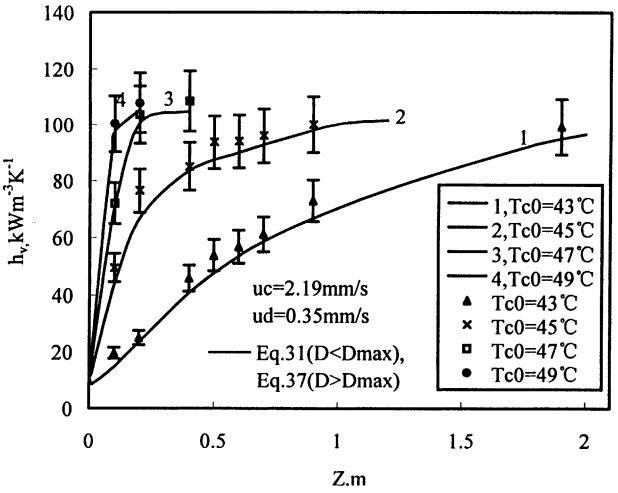

Fig. 4. Variation of h_v with Z for specific values of u_c and u_d.

$$h_{vi} = \frac{8\rho_c V_{ci} C_{pc}(T_{c(i-1)} - T_{ci})}{\pi D_r^2\,\Delta Z_i(\Delta T_{(i-1)} + \Delta T_i)} \tag{41}$$

where i is the ith element of volume.

With the experimentally determined distribution of temperature, pressure and gas hold-up along the exchanger height at different experimental conditions, the value of h_{vi} in the gas–liquid–liquid three-phase section of the exchanger can be calculated by using Eq. (41). Figs. 4–6 indicate the effects of the main operational parameters on the volumetric heat transfer coefficient. In these figures, the dispersed points are the experimental values of h_v and the curves are the theoretical values. The theoretical values are calculated by Eq. (31) when D is less than D_{max} and are calculated by Eq. (37) when D is larger than D_{max}.

4.1. Effects of T_{c0} on h_v

The effects of the initial temperature of the continuous phase on the volumetric heat transfer coefficient are shown

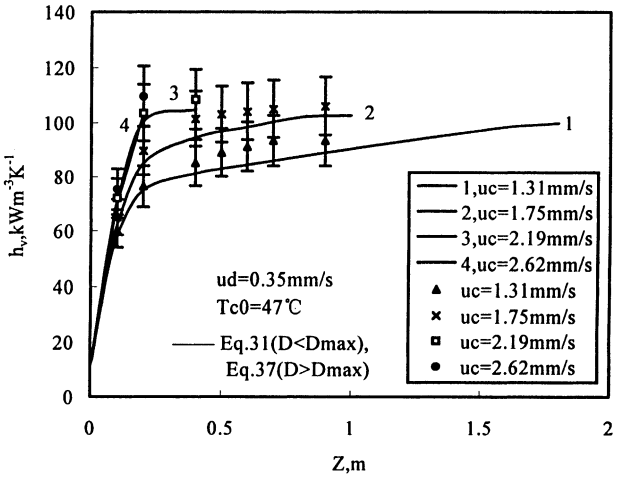

Fig. 5. Variation of h_v with Z for specific values of u_d and T_{c0}.

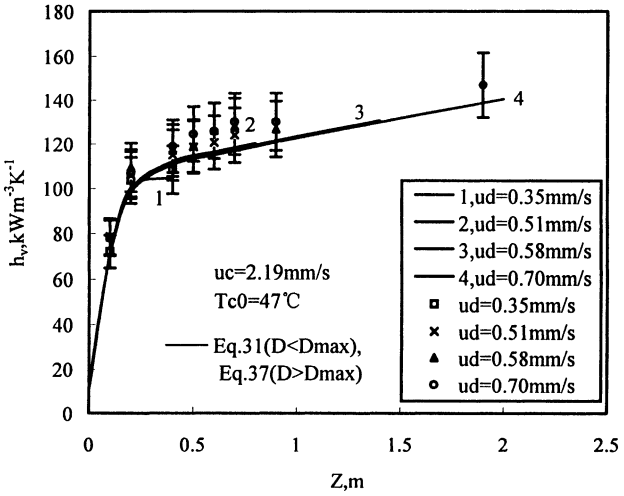

Fig. 6. Variation of h_v with Z for specific values of u_c and T_{c0}.

in Fig. 4. The figure shows the variations of h_v along the axis at $T_{c0} = 43.00$, 45.00, 47.00, 49.00°C, respectively, while $u_c = 2.19$ and $u_d = 0.35\,\mathrm{mm\,s^{-1}}$. As is seen from the figure, the volumetric heat transfer coefficient, h_v, increases greatly when the continuous phase inlet temperature increases, and it increases with an increase in axial height for a given initial temperature. Furthermore, there is a rapid increase of h_v along the axis at the lower part of the exchanger. The higher the initial temperatures of the continuous phase the clearer this trend. This is the result of the increase of the two-phase droplets' diameter and number when T_{c0} increases. Because the increase of T_{c0} enlarges the temperature driving force and leads to the rapid evaporation of the dispersed phase liquid, the diameter (in the first stage) or the number density of the two-phase droplets (in the second stage) will become larger for an exchanger height. At the same time, the volumetric heat transfer coefficient defined by Eq. (31) and (37) is directly proportional to the diameter and the number density of two-phase droplets. The h_v will certainly increase with the increase of T_{c0}. When the two-phase droplets evaporate to the degree that it is not enough for the dispersed liquid to form a film on the inside surface of the droplets [17], the effective surface for heat transfer will not increase linearly with the surface of the droplets. Then with the increase of the axial height, the increase of h_v will become slowly. Accordingly, the slope of each curve will also decrease gradually. From this figure, we also see that the height required for the complete evaporation of the dispersed phase, H_v, decreases with the increase of T_{c0} because of the increase of the temperature driving force that leads to the increase of the heat transfer rate between the continuous and dispersed phases.

4.2. Effects of u_c on h_v

Fig. 5 shows the effects of the continuous phase superficial velocity on the volumetric heat transfer coefficient at $u_d = 0.35\,\mathrm{mm\,s^{-1}}$ and $T_{c0} = 47.00$°C. Lines 1, 2 and 3 indicate that h_v increases with the increase of u_c at a certain height. That is to say, when the ratio of the continuous phase superficial velocity to the dispersed phase superficial velocity is less than about 6.0, the increase of u_c can lead to the increase of h_v. The reason is that with the increase of u_c, more heat can be supplied for the evaporation of the dispersed phase. Then, supplying the same heat for the dispersed phase, the temperature of the continuous liquid will be higher correspondingly at a certain axial height for the higher u_c. This has the same effects as the increase of the temperature driving force. So the curves in Fig. 5 are similar to those in Fig. 4. The distributions of h_v along the axis vary from logarithmic increase to linear increase with the increase of u_c and the H_v also becomes lower. But when the ratio of u_c to u_d is larger than 6.0, for example lines 3 and 4 in Fig. 5, the continuous phase superficial velocity nearly has no effects on h_v. Because when u_c increases to a certain extent, supplying the same heat for the dispersed phase, the difference of the continuous liquid temperature at a given height for the different u_c will be very small. Accordingly, the temperature driving force will also nearly have no changes. Then, according to the discussions in Section 4.1 the change of u_c that has increased to that extent will nearly have no effects on h_v.

4.3. Effects of u_d on h_v

From Fig. 6 we can see the effects of u_d on h_v at $u_c = 2.19\,\mathrm{mm\,s^{-1}}$ and $T_{c0} = 47.00$°C. The superficial velocity of the dispersed phase nearly has no effect on h_v. This is the result of the interaction of n_{d0}, D, ΔT, Z on h_v. Their relationship is defined by Eq. (31) or Eq. (37). Since the change of the volumetric heat transfer coefficient is inconsiderable, the increase of u_d means the increase in height for the dispersed phase evaporating completely. So it can be seen that the height required for the complete evaporation of the dispersed phase increases correspondingly with the increase of u_d in Fig. 6.

Figs. 4–6 show that the continuous lines lie below data points. The mainly reason is that the rate of heat released to the environment, Q_e, is not considered in calculating the experimental values of h_v by Eq. (41). In this equation the item of $\rho_c V_{ci} C_{p_c}(T_{c(i-1)} - T_{ci})$ is the rate of heat flow out from the continuous liquid and the item of $(1/4)\pi D_r^2 h_{vi}\,\Delta Z_i((\Delta T_{(i-1)} + \Delta T_i)/2)$ is the rate of heat flow entering into the dispersed liquid. If Q_e is considered, Eq. (41) would be

$$h_{vi} = \frac{8[\rho_c V_{ci} C_{p_c}(T_{c(i-1)} - T_{ci}) - Q_e]}{\pi D_r^2\,\Delta Z_i(\Delta T_{(i-1)} + \Delta T_i)} \tag{42}$$

Because the value of Q_e is small, Q_e is neglected in Eq. (41). Then, the value of h_v calculated by Eq. (41) will be higher than that by Eq. (42). Accordingly, the values of the data points are little bigger than that of the continuous lines. Figs. 4–6 also show a good agreement of the theoretical values of h_v with the experimental values.

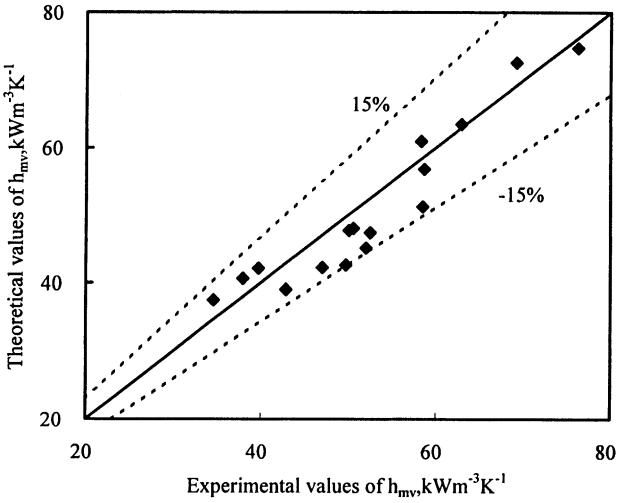

Fig. 7. Comparison of theoretical and experimental values of h_{mv}.

4.4. Comparison of theoretical and experimental values of h_{mv}

Fig. 7 shows the comparison of theoretical and experimental values of the average volumetric heat transfer coefficient. The theoretical values are calculated by Eqs. (33) and (39). The experimental average volumetric heat transfer coefficient in the gas–liquid–liquid three-phase section can be calculated by

$$h_{mv} = \frac{\sum \Delta T_i \, h_{vi} \, \Delta Z_i}{\Delta T_{av} \, H_v} \tag{43}$$

The figure shows that errors between the theoretical and experimental values are within 15% for the different experimental conditions. It indicates that the models we have derived are reliable. The errors are mainly caused by the following reasons. One is the assumption of linear distribution in temperature driving force. The other is the assumption that the relative velocity is constant. The third is the uncertainties in the experimental measurements and the transport property values.

5. Conclusions

1. The effects of the operational parameters on the volumetric heat transfer coefficient were studied. The results indicated that the volumetric heat transfer coefficient, h_v, increased with the increase of the initial temperature, T_{c0}, and the superficial velocity of continuous liquid u_c, while the superficial velocity of dispersed liquid, u_d, nearly had no effects on it.
2. The exchanger was divided into two zones according to the maximum diameter that the droplet can attain. The mathematical models for the local and average volumetric heat transfer coefficient were obtained for each zone. Finally, the theoretical values were compared to the experimental values and the results were satisfactory.

References

[1] L. Yongcheng, L. Changhou, S. Ziqiu, Heat transfer in bubble column and gas-lift loop reactors, J. Eng. Thermophys. 10 (1989) 72–74.
[2] K.S. Spiegler, Principles of Desalination, Academic Press, New York, 1966.
[3] L.W. Byrd, J.C. Mulligan, A population balance approach to direct-contact secondary refrigerant freezing, AIChE J. 32 (1986) 1881–1894.
[4] Q. Tao, L. Chunxiang, S. Ziqiu, Vaporizing cooling heat transfer of the alcohol liquid drops in sucrose solution and crystallization process, J. Chem. Eng. Chin. Univ. (China) 11 (1997) 37–42.
[5] H.R. Jacobs, Direct-contact heat transfer for process technologies, J. Heat Transfer 110 (1988) 1259–1270.
[6] S.B. Plass, H.R. Jacobs, R.F. Boehm, Operation characteristics of a spray column type direct-contact preheater, AIChE Symp. Ser. 189 (1979) 227–234.
[7] R.C. Smith, W.M. Rohsenow, M.S. Kazimi, Volumetric heat transfer coefficient for direct-contact evaporation, Trans. ASME J. Heat Transfer 104 (1982) 264–270.
[8] K.L. Core, J.C. Mulligan, Heat transfer and population characteristics of dispersed evaporating droplets, AIChE J. 36 (1990) 1137–1144.
[9] M. Sevik, S.H. Park, The splitting of drops and bubbles by turbulent fluid flow, Trans. ASME J. Fluid Eng. 95 (1973) 53–60.
[10] D.A. Lewis, J.F. Davidson, Bubble sizes produced by shear and turbulence in a bubble column, Chem. Eng. Sci. 38 (1983) 161–167.
[11] M.A. Young, R.G. Carbonell, D.F. Ollis, Airlift bioreactor: analysis of local two-phase hydrodynamics, AIChE J. 37 (1991) 403–428.
[12] Z. Peng, W. Kun, W. Yiping, The fluid dynamics model of gas–liquid–liquid three-phase flow, J. Chem. Eng. Chin. Univ. (China) 14 (2000) 25–30.
[13] Y.H. Mori, An analytic model of direct-contact heat transfer in spray-column evaporators, AIChE J. 37 (1991) 539–546.
[14] Y. Shimizu, Y.H. Mori, Evaporation of single liquid drops in an immiscible liquid at elevated pressures: experimental study with *n*-pentane and R113 drops in water, Int. J. Heat Mass Transfer 31 (1988) 1843–1851.
[15] K.N. Seetharamu, P. Battya, Direct-contact evaporation between two immiscible liquids in a spray column, Trans. ASME J. Heat Transfer 111 (1989) 780–785.
[16] T. Coban, R. Boehm, Performance of a three-phase, spray-column, direct-contact heat exchanger, Trans. ASME J. Heat Transfer 111 (1989) 166–172.
[17] H.C. Simpson, G.C. Beggs, M. Nazir, Evaporation of butane drops in brine, Desalination 15 (1974) 11–24.